ASIAN JOURNAL OF PHARMACEUTICAL SCIENCES 9 (2014) 191–198

Available online at www.sciencedirect.com

ScienceDirect

journal homepage: http://ees.elsevier.com/ajps/default.asp

Original Research Paper

Polyelectrolyte complex micelles by self-assembly of polypeptide-based triblock copolymer for doxorubicin delivery

*Jeong Hwan Kim, Thiruganesh Ramasamy, Tuan Hiep Tran, Ju Yeon Choi, Hyuk Jun Cho, Chul Soon Yong**, Jong Oh Kim**

College of Pharmacy, Yeungnam University, 214-1, Dae-Dong, Gyongsan 712-749, South Korea

ARTICLE INFO

Article history:
Received 2 March 2014
Received in revised form
29 April 2014
Accepted 3 May 2014
Available online 16 May 2014

Keywords:
Polyelectrolyte
Micelles
Drug delivery
Poly(L-aspartic acid)
Poly(ethylene glycol)

ABSTRACT

Polyelectrolyte complex micelles were prepared by self-assembly of polypeptide-based triblock copolymer as a new drug carrier for cancer chemotherapy. The triblock copolymer, poly(L-aspartic acid)-*b*-poly(ethylene glycol)-*b*-poly(L-aspartic acid) (PLD-*b*-PEG-*b*-PLD), spontaneously self-assembled with doxorubicin (DOX) via electrostatic interactions to form spherical micelles with a particle size of 60–80 nm (triblock ionomer complexes micelles, TBIC micelles). These micelles exhibited a high loading capacity of 70% (w/w) at a drug/polymer ratio of 0.5 at pH 7.0. They showed pH-responsive release patterns, with higher release at acidic pH than at physiological pH. Furthermore, DOX-loaded TBIC micelles exerted less cytotoxicity than free DOX in the A-549 human lung cancer cell line. Confocal microscopy in A-549 cells indicated that DOX-loaded TBIC micelles were transported into lysosomes via endocytosis. These micelles possessed favorable pharmacokinetic characteristics and showed sustained DOX release in rats. Overall, these findings indicate that PLD-*b*-PEG-*b*-PLD polypeptide micelles are a promising approach for anti-cancer drug delivery.

1. Introduction

Doxorubicin (DOX) is a widely used chemotherapeutic agent that is highly effective against a range of tumors, including breast, ovarian, lung, and thyroid cancer. However, its therapeutic effects have been limited by its poor pharmacokinetic profile and its severe adverse effects, including cardiomyopathy and congestive heart failure [1–4]. Thus, a smart drug delivery system is needed to maximize the therapeutic

* *Corresponding author*. Tel.: +82 53 810 2813; fax: +82 53 810 4654.
** *Corresponding author*. Tel.: +82 53 810 2812; fax: +82 53 810 4654.
E-mail addresses: csyong@yu.ac.kr (C.S. Yong), jongohkim@yu.ac.kr (J.O. Kim).

Peer review under responsibility of Shenyang Pharmaceutical University

Production and hosting by Elsevier

http://dx.doi.org/10.1016/j.ajps.2014.05.001

efficacy of DOX and minimize its systemic toxicity by selective tumor delivery [1,3].

Although a wide range of drug delivery systems is available, polymer-based drug delivery systems have attracted attention owing to their small size and their ability to contain a wide range of therapeutic agents [5]. Nanoscale polymeric micelles have several beneficial features, including long blood circulation times, avoidance of renal excretion, and passive targeting via the enhanced permeability and retention effect (EPR effect) [6,7].

Recently, nanofabrication of polymeric micelles has been considerably advanced by the use of block copolymers containing ionic and nonionic blocks ("block ionomers") [8,9]. Such block copolymers react with oppositely charged species through electrostatic interaction, resulting in block ionomer complexes (BIC). Neutralization of ionic chains leads to the formation of hydrophobic segments, which facilitate generation of nano-sized particles. Furthermore, BIC possess a core–shell architecture, with the drug incorporated in a hydrophobic core palisaded by hydrophilic and nonionic chains, generally poly(ethylene glycol) (PEG) [10,11]. The PEG corona prevents nanoparticles from being captured by reticuloendothelial systems (RES) and from aggregation, ensuring their *in vivo* longevity [12–14]. The small size of the BIC micelles leads to extravasation, enabling penetration into tissues and cells. BIC micelles have been intensively investigated because of their ability to carry low-molecular-weight drugs [15], proteins [16,17], genes [18], and imaging agents [19–21]. In particular, polypeptide-based block ionomers have been extensively explored as effective drug delivery systems for anti-cancer drugs, owing to their biocompatibility, biodegradability, and lack of toxicity [22–25].

Various polypeptide-based polymers have been synthesized and investigated in recent years [21,26–28]. However, the majority of studies have been of diblock copolymers and there have been fewer investigations of triblock copolymers. The present study therefore explored the polypeptide-based triblock copolymer, poly(L-aspartic acid)-*b*-poly(ethylene glycol)-*b*-poly(L-aspartic acid) (PLD-*b*-PEG-*b*-PLD), to develop a biodegradable nanocarrier for the delivery of anti-cancer drugs. We prepared triblock ionomer complex micelles (TBIC micelles) and evaluated their physicochemical properties, as well as their DOX-loading efficiencies and *in vitro* release behaviors in different pH environments. We also investigated the cytotoxicity of DOX delivered using TBIC micelles and the pharmacokinetics of DOX-containing TBIC micelles in an *in vivo* animal model.

2. Materials and methods

2.1. Materials

Poly(L-aspartic acid)-*b*-poly(ethylene glycol)-*b*-poly(L-aspartic acid) (PLD-*b*-PEG-*b*-PLD) triblock copolymers (M_w/M_n = 1.20, Mw = 7700) were purchased from Alamanda Polymers, Inc. (Huntsville, AL, USA). The block lengths were 114 and 10 repeating units for PEG and PLD, respectively. Doxorubicin HCl (DOX) was kindly provided by Dong-A Pharmaceutical Company (Yongin, Korea). A-549 cells were obtained from the Korean Cell Line Bank (Seoul, Korea). MTT reagent (3-(4,5-dimethylthiazol-2-yl)-2,5-diphenyltetrazolium bromide) and paraformaldehyde were purchased from Sigma–Aldrich (St Louis, MO, USA). Lysotracker® green and dimethyl sulfoxide (DMSO) solution were obtained from Invitrogen Inc. (Carlsbad, CA, USA) and Applichem (Darmstadt, Germany), respectively. RPMI 1640, penicillin and streptomycin, and heat-inactivated fetal bovine serum (FBS) were supplied by Hyclone (Logan, UT, USA). All other reagents were of analytical grade and used without further purification.

2.2. Preparation of polyelectrolyte complex micelles

TBIC micelles were prepared by polyion complexation of the anionic triblock copolymer PLD-*b*-PEG-*b*-PLD and cationic DOX via electrostatic interactions. DOX (1 mg/mL) and PLD-*b*-PEG-*b*-PLD (1 mg/mL) were dissolved separately in distilled water. These two aqueous solutions were then mixed, with the molar ratio of DOX to carboxylate groups in the micelle (R = [DOX]/[COOH]) ranging from 0.25 to 0.5 [15]. Unbound DOX was removed by ultrafiltration by using Amicon® Ultracel centrifugal filter devices (molecular weight cut-off, 10,000 Da; Millipore, Billerica, MA, USA) pretreated with free DOX [4]. The DOX concentration in the filtrates was determined by measuring the absorbance at 480.5 nm by using a UV/Vis spectrophotometer (U-2800, Hitachi, Japan) [4].

2.3. UV/Vis and fluorescence studies

A UV/Vis spectrometer was used to conduct a wavelength scan of the free drug and TBIC micelles. An aqueous solution of DOX was screened, followed by a scan of DOX-loaded TBIC micelle solutions over a wavelength range of 200 nm–650 nm.

The fluorescent spectra of free DOX and TBIC micelles were analyzed using a fluorescence spectrometer (LS 55, PerkinElmer, USA). The data were recorded using an excitation wavelength of 480 nm and a bandwidth of 5 nm for excitation and emission. All measurements were conducted at room temperature, and the concentration of DOX was constant in all the samples.

2.4. Drug loading

Drug loading was assessed using UV/Vis spectrophotometry. Unbound DOX was removed by ultrafiltration, and the micellar drug concentration was determined by measuring the absorbance of filtrates at 480.5 nm. Loading capacity (%) and loading efficiency (%) were calculated as follows:

$$\text{Loading capacity (\%)} = \frac{(\text{DOX}_{\text{total}} - \text{DOX}_{\text{unbound}})}{(\text{Micelle}_{\text{total}})} \times 100$$

$$\text{Loading efficiency (\%)} = \frac{(\text{DOX}_{\text{total}} - \text{DOX}_{\text{unbound}})}{(\text{DOX}_{\text{total}})} \times 100$$

where $\text{DOX}_{\text{total}}$, $\text{DOX}_{\text{unbound}}$, and $\text{Micelle}_{\text{total}}$ are the total amount of DOX added, unbound DOX, and micelles respectively.

2.5. DLS characterization

The hydrodynamic particle sizes, polydispersity index (PDI), and ζ-potential of the TBIC micelles were measured by dynamic light scattering (DLS) using the Zetasizer Nano S90 (Malvern Instruments, Worcestershire, UK) with an He-Ne laser source, operating at a wavelength of 633 nm with a 90° scattering angle. The hydrodynamic size, PDI, and ζ-potential were determined using the Nano DTS software (version 6.34) provided by the manufacturer. All measurements were performed at room temperature, and mean values were calculated following measurement of at least three sets of ten runs.

2.6. Morphological analysis

The morphologies of TBIC micelles were observed by transmission electron microscopy (TEM; H-7600, Hitachi, Tokyo, Japan) at an accelerating voltage of 100 kV. The micelles were stained with 2% (w/v) phosphotungstic acid, dropped onto copper grids with films, air-dried under an infrared lamp for 10 min, and observed using TEM.

2.7. In vitro drug release studies

The release profiles of DOX from TBIC micelles were studied in phosphate-buffered saline (PBS, pH 7.4, 0.14 M NaCl) and acetate buffered saline (ABS, pH 5.0, 0.14 M NaCl) by dialysis with a molecular weight cut-off of 3.5 kDa (Spectrum Laboratories, CA, USA). The experiments were performed in a shaking water bath maintained at 37 °C and 100 rpm. At specified time intervals (1–48 h), 5 mL of sample was withdrawn from tubes containing 30 mL release medium, and replaced with an equal volume of fresh buffer solution. The collected samples were analyzed using a spectrophotometer to determine the concentration of DOX by measuring absorbance at 480.5 nm. The amount of DOX in the dialysis bag was equal for every sample, and the experiment was conducted in triplicate under each condition. The amount of DOX released was expressed as a percentage of the total DOX and plotted as a function of time.

2.8. In vitro cytotoxicity assay

The *in vitro* cytotoxicity of free DOX and TBIC micelles in the A-549 human lung cancer cell line was assessed using the MTT assay. In brief, 1×10^4 A-549 cells were seeded in 96-well plates and allowed to attach for 24 h at 37 °C. The cells were treated with free DOX or TBIC micelles for 24 h at 37 °C. To assess the toxicity of the polymer itself, PLD-*b*-PEG-*b*-PLD aqueous solutions were also incubated with A-549 cells in separate plates. After treatment for 24 h, the cells were washed twice with PBS and maintained in RPMI medium with 10% FBS for additional 72 h. The cells were then incubated with 100 μl of MTT solution (1 mg/mL) for 3 h before adding DMSO (100 μl) to dissolve the MTT formazan crystals. The absorbance at 570 nm was measured with a microplate reader (Multiskan EX, Thermo Scientific, USA). All measurements were performed eight times. The cell viability (%) was calculated using the following equation:

$$\text{Cell viability } (\%) = (A_{\text{sample}}/A_{\text{control}}) \times 100$$

where A_{sample} and A_{control} were the absorbance of the sample (treated cells) and the control (untreated cells), respectively. IC_{50} values (the concentration that caused 50% reduction in cell viability) were calculated using GraphPad Prism ver. 5.0 (GraphPad Software, San Diego, CA).

2.9. Cellular uptake study

The cellular uptake of TBIC micelles was investigated using confocal laser scanning microscopy. A-549 cells at 70–80% confluency were trypsinized and seeded on coverslips in a 12-well plate at a density of 1.0×10^5 cells/well. After 24 h, cells were treated with free DOX or TBIC micelles (5 μg/mL) for 30 min. The cells were then washed three times with PBS solution before staining with Lysotracker® green DND-26 (100 nM) for 10 min. The cells were again washed twice with PBS, fixed for 15 min with 4% paraformaldehyde at room temperature, and rinsed with 4 °C PBS solution. Subsequently, the coverslips were taken out of the wells, carefully mounted on glass slides with one drop of gel/mount solution (M01, Biomeda, USA), sealed with nail polish, and observed by confocal laser scanning microscopy (Nikon A1, Japan).

2.10. In vivo pharmacokinetic studies

2.10.1. Animals

The experimental protocols for the animal studies were approved by the Institutional Animal Ethical Committee, Yeungnam University, South Korea. Male Sprague–Dawley rats (250 ± 10 g; 8 weeks) (Orient Bio. Inc., Seungnam, South Korea) were fasted for 12 h prior to the experiments.

2.10.2. Administration and blood collection

The rats were divided into three groups and anesthetized with diethyl ether. The right femoral artery of each rat was cannulated with a polyethylene tube (PE-50, BD, Maryland, USA). The tube was flushed with 0.3 mL of heparinized normal saline solution (100 IU) to prevent blood clotting. Free DOX solution or TBIC micelle solution was administered intravenously at a dose of 10 mg/kg as DOX. Blood samples (250 μl) were collected from the left femoral artery at specified intervals. The samples were centrifuged at 13,000 rpm for 10 min to obtain a plasma supernatant for further analyses.

2.10.3. Blood sample analysis

Plasma DOX concentration was analyzed by high-performance liquid chromatography (HPLC) using previously reported methods, with slight modification [29]. Briefly, 150 μl of plasma was deproteinized by mixing with 150 μl of methanol, followed by vortexing and mild bath sonication for 5 min. The samples were then centrifuged at 13,000 rpm for 10 min. The supernatant was separated and evaporated in a centrifugal evaporator (Modul 3180C, Biotron, South Korea). The residue was reconstituted in 100 μl of methanol and quantified by HPLC (Hitachi, Japan) with an Inertsil® ODS-3 column (GL Science, 5 μm, 4.6 × 150 mm). The mobile phase was composed of methanol/water/acetic acid at a volume ratio of 50/49/1 (pH 2.9), with a flow rate of 1.0 mL/min. The UV/Vis detector (Model L-2420) was set at 254 nm. Pharmacokinetic parameters such as the area under the drug

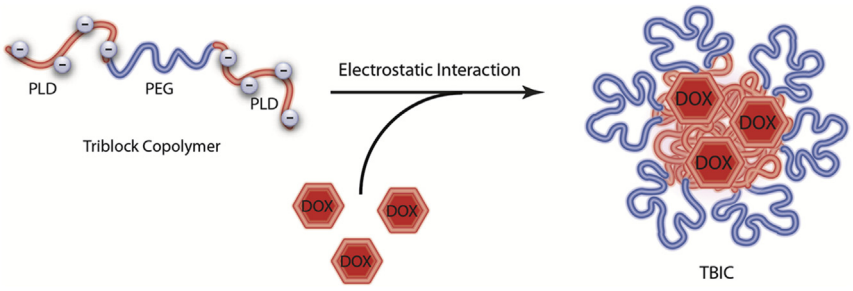

Fig. 1 – Schematic illustration of the formation of TBIC micelles.

concentration-time curve from 0 to 24 h (AUC), elimination rate constant (K_{el}), and half-life ($t_{1/2}$) were calculated using non-compartmental analysis (WinNolin® software; professional edition, version 2.1; Pharsight Co., CA, USA). Levels of statistical significance were assessed using analysis of variance (ANOVA). Differences were considered to be statistically significant when $P < 0.05$. All data were expressed as mean ± standard deviation (SD).

3. Results and discussion

3.1. *Preparation of TBIC micelles*

DOX-loaded TBIC micelles were formed by ionic complexation between anionic PLD-*b*-PEG-*b*-PLD polymers ($pK_a = 4.0$) and cationic DOX ($pK_a = 8.3$), as shown in Fig. 1. Electrostatic interactions allowed DOX to be immobilized in the cores of these TBIC micelles [15]. The micelles were formulated at [DOX]/[COOH] molar ratios (*R*) ranging from 0.25 to 0.5. Fig. 2 shows the average particle sizes, PDI, and ζ-potential of TBIC micelles ($R = 0.25$ and 0.5) at various pH. At the lower drug:polymer ratio of $R = 0.25$ and pH 7, TBIC micelles showed much smaller particle size (~60 nm). However, at $R = 0.5$, slight increases in particle size of TBIC micelles were observed at all pH studied. This is because the increased hydrophobicity in TBIC micelles with a high *R* value induced slight aggregation, which can cause the increased size. Notably, there was no precipitation of TBIC micelles in aqueous solutions. In all cases, every mixture had a nanometer-scale size and low PDI of approximately 0.2. In addition, PEG segments prevented the agglomeration of nanoparticles via steric repulsion and decreased micelle hydrophobicity [15,30]. It is also worth noting that increased acidity of the mixture was associated with increased particle hydrodynamic diameter. This was owing to a reduction in the level of deprotonated forms of the PLD blocks, and the resulting reduction in the binding force driving complex formation [5]. The ζ-potential values of TBIC micelles are presented in Fig. 2C. At $R = 0.25$ and 0.5, an increase in the amount of DOX added to PLD-*b*-PEO-*b*-PLD resulted in an increase in ζ-potential. Compared to $R = 0.25$, the ζ-potential of TBIC micelles at $R = 0.5$ showed slightly lower negativity. This was because of the different degree of neutralization by the increased amount of DOX in the complex.

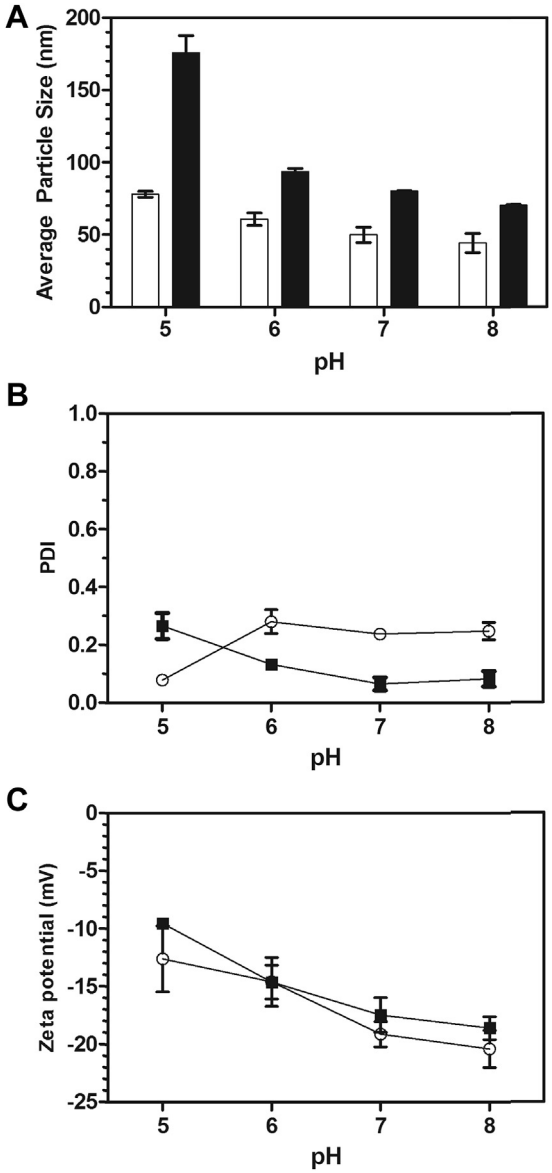

Fig. 2 – (A) Average hydrodynamic diameter, (B) PDI, and (C) ζ-potential of TBIC micelles at various pH and compositions (*R*). *R* = 0.25, white bar or open circles; *R* = 0.50, black bar or filled squares. The data are presented as mean ± SD ($n = 3$).

UV/Vis spectroscopy was employed to investigate the physicochemical interactions between DOX and polymers. A chromophore, composed of three aromatic hydroxyanthraquinonic rings in the structure of DOX, was used to clarify its interactions with other molecules [31]. As depicted in Fig. 3A, the UV/Vis spectra of free DOX and TBIC micelles revealed only slight differences in the visible absorption spectrum. However, the presence of a redshift in the absorption peaks was clearly indicative of DOX–DOX interactions, through π-π stacking effects [22,31–33]. Furthermore, the increased local concentration of DOX in the core of TBIC micelles resulted in decreased absorbance. Fluorescent spectra provided more information (Fig. 3B), with a significant decrease in fluorescence intensity observed in the DOX from TBIC micelles, compared to that in free solution at the same concentration. This reduction in DOX fluorescence intensity could be attributed to the location of the DOX molecules, which were bound to the deprotonated COOH group in the PLD chain within the micelle core [15,24]. The quenched DOX fluorescence therefore indicated that DOX had been successfully incorporated into the TBIC micelle core.

TEM images revealed the structural morphology of the TBIC micelles (Fig. 4), which clearly showed spherical particles

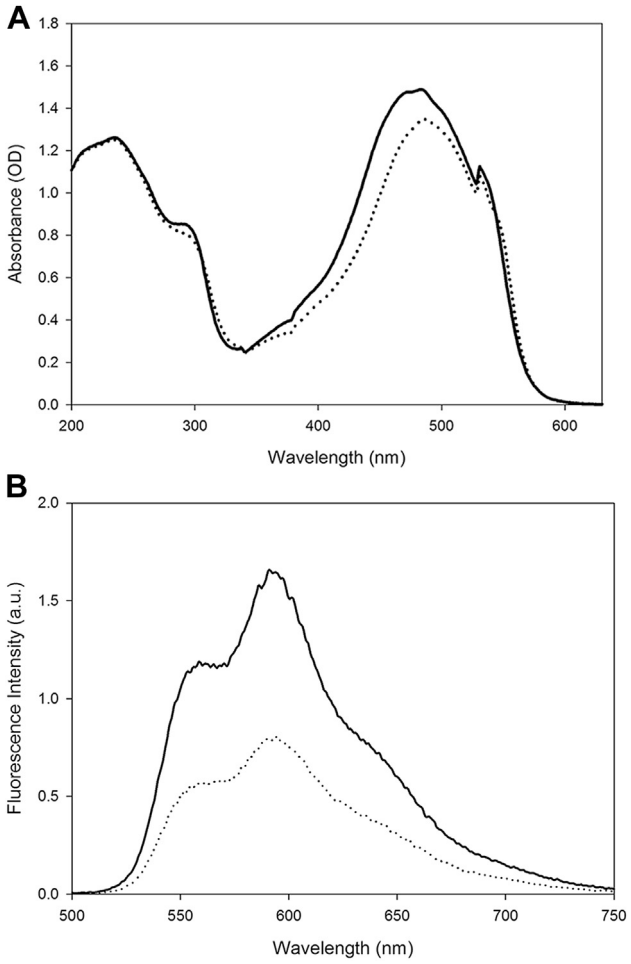

Fig. 3 – (A) UV/Vis spectra, and (B) fluorescence emission spectra of free DOX (—) and TBIC micelles (·····). Concentration of DOX is 50 μg/mL.

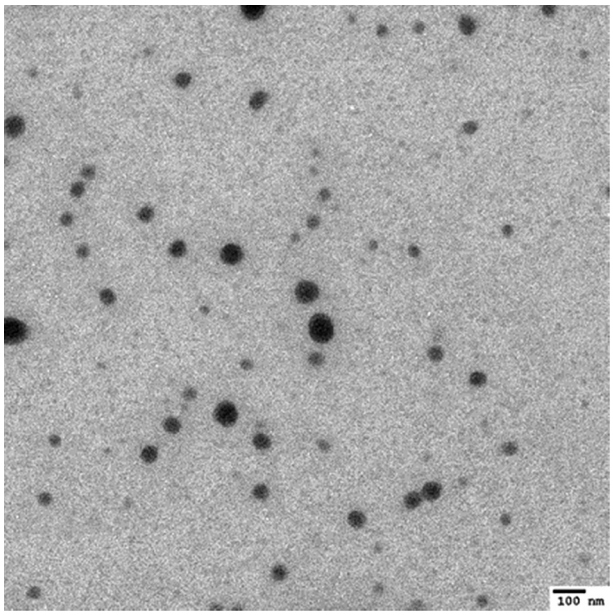

Fig. 4 – Transmission electron microscopy images of TBIC micelles. The length of the scale bar was 100 nm at 10,000 × magnification.

with core–shell structure. These showed good particle integrity, suggesting strong interactions between PLD and DOX. The high contrast cores, which consisted of the hydrophobic PLD/drug complex, were surrounded by a gray boundary, indicating the PEG blocks. The narrowly distributed TBIC micelles had particle sizes of less than 100 nm, corresponding well to the DLS data.

3.2. *Drug loading and* in vitro *release study*

The loading capacity and efficiency of TBIC micelles at various molar ratios were measured by UV/Vis spectroscopy. The DOX loading capacities of TBIC micelles were 36.8 ± 1.5 w/w% and 69.4 ± 4.7 w/w% for $R = 0.25$ and 0.5, respectively. In all complexes, the loading efficiencies of DOX were maintained above 90%. It is worth noting that the DOX payload in the micelles was doubled by increasing R from 0.25 to 0.50. This phenomenon might indicate that all the additional DOX interacted with unoccupied carboxylic groups in the polymer, without exception. Hence, $R = 0.50$ was selected as the optimized ratio for further experiments.

The DOX release profiles were investigated by equilibrium dialysis of the micelles at 37 °C at pH 7.4 or pH 5.0 (Fig. 5). At physiological pH 7.4, TBIC micelles showed a significantly prolonged release profile up to 48 h, with only ~34% of the loaded DOX released during the first 10 h. The majority of the loaded DOX (about 60%) was still immobilized in the core of TBIC micelles after 48 h [4,31]. In contrast, the release profiles dramatically changed at the weakly acidic pH 5.0. During the first 8 h at pH 5.0, almost 80% of DOX was liberated from the TBIC micelles. This accelerated release of DOX was attributable to the protonation of carboxylic groups in polymer PLD

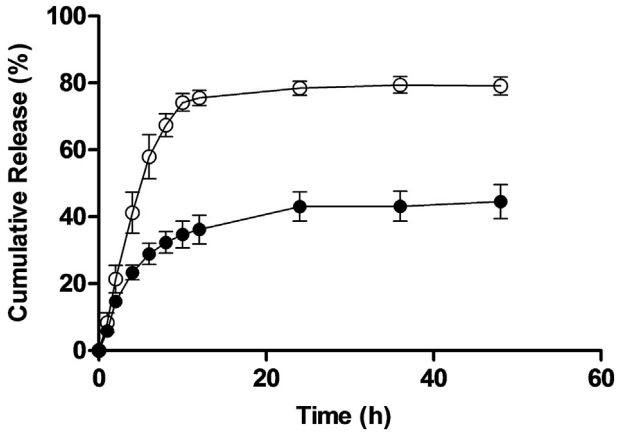

Fig. 5 – *In vitro* DOX release profiles from TBIC micelles at pH 7.4 (●) and pH 5.0 (○). Micelles were prepared at R = 0.5, and pH 7.0. The loading amount of DOX for each sample is 200 μg. The data are presented as mean ± SD (*n* = 3).

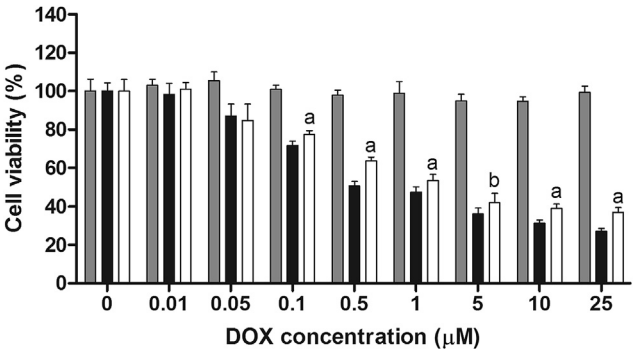

Fig. 7 – *In vitro* cytotoxicity of free DOX (black bar), TBIC micelles (white bar), and free polymer (gray bar) in A-549 cells. TBIC micelles was prepared at R = 0.5, and pH 7.0. The data are presented as mean ± SD (*n* = 6). a: *P* < 0.01 compared to free DOX. b: *P* < 0.05 compared to free DOX.

chains, resulting in weak electrostatic interactions between DOX and PLD [4,15,34]. As reported previously, extraordinarily low pH (pH 5.7–7.2) is a phenotype distinguishing solid tumors from the surrounding tissues [31,35]. In addition, more acidic conditions can be found in endosomes (pH 5–6) and lysosomes (pH 4–5) [3,35]. Therefore, this pH-sensitive release of micelles could be triggered when the nanoparticles encounter acidic environments of cancerous sites or cell organelles.

3.3. In vitro *cellular uptake and cytotoxicity*

Cellular uptake of DOX in the human A-549 cell line was characterized using confocal laser scanning microscopy. Previous studies have shown that BIC micelles based on polypeptides enter cancer cells via endocytosis, subsequently moving from endosomes to lysosomes [2,36,37]. Similarly, TBIC micelles exhibited a high level of co-localization with lysosomes in A-549 cells within 30 min (Fig. 6). In contrast, free DOX (control) was only detected in the nuclei, and no co-localization was observed. This phenomenon highlighted the feasibility of lysosomal pH-triggered DOX release from BIC micelles, as well as degradation of the carrier at the cellular level.

Fig. 7 shows the cytotoxicity of DOX-loaded TBIC micelles in the A-549 cell line, as observed using the MTT assay. Cell viability was progressively reduced in a TBIC micelle dose-dependent manner, although the micelles showed significantly less cytotoxicity than that shown by free DOX. The reduced cytotoxic activity of TBIC micelles resulted from the more sustained release of DOX from these micelles. Importantly, polymer (PLD-*b*-PEG-*b*-PLD) did not have any influence on cell viability over the entire range of concentrations used for the treatment. These results suggested that tri-block copolymer was biocompatible.

3.4. *Pharmacokinetic study*

The plasma concentration-time profiles of DOX after intravenous injection of DOX solution and DOX-loaded TBIC micelles at a dose of 10 mg/kg to rats are shown in Fig. 8 and the relevant pharmacokinetic parameters are listed in Table 1. Administration of TBIC micelles produced a markedly higher DOX concentration than did free DOX administration, which

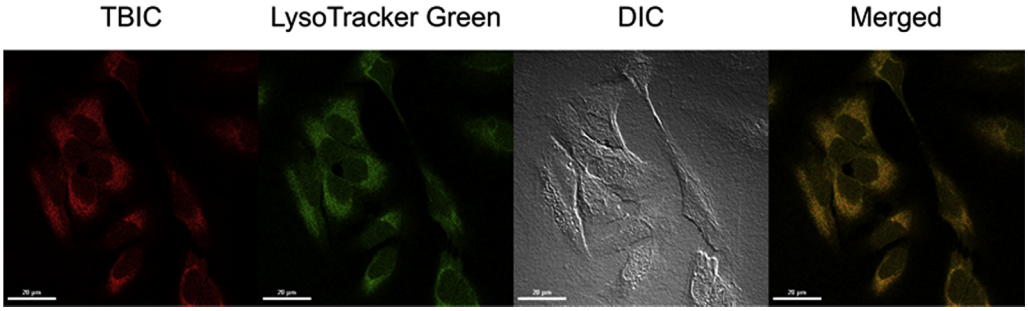

Fig. 6 – *In vitro* cellular uptake studies of TBIC micelles in A-549 human lung cancer cells. A-549 cells were exposed for 30 min at 37 °C to TBIC micelles and Lysotracker® (Green) for 10 min. Images show significant co-localization of TBIC micelles within the lysosomes.

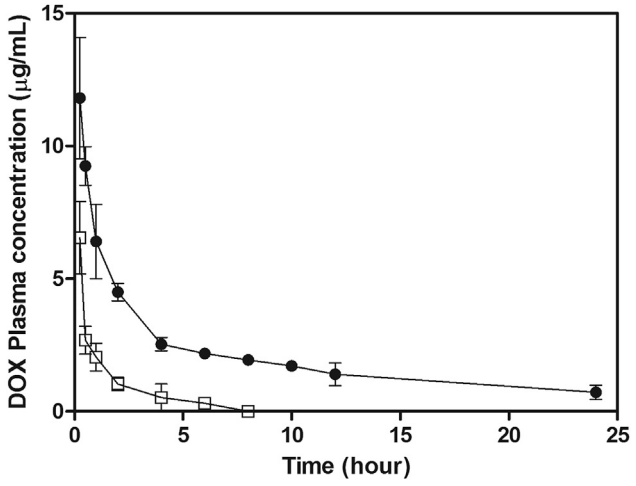

Fig. 8 – *In vivo* pharmacokinetic profiles after intravenous administration of free DOX (□) and TBIC micelles (●) in rats at a dose of 10 mg/kg. TBIC micelles were prepared at R = 0.5, and pH 7.0. The data are presented as mean ± SD (*n* = 3).

was immediately removed from the circulation after administration. Compared to the free DOX solution, DOX delivery using TBIC micelles resulted in a 7-fold increase in $t_{1/2}$ and AUC_{all}, and a 7-fold decrease in clearance. These *in vivo* pharmacokinetic characteristics of DOX from the TBIC micelles were understood to be related to the longevity of the nanoparticles in the circulation.

The major advantages of polymeric micelles as circulating drug carriers are that non-specific interactions with healthy tissues and premature clearance by RES are hindered by steric repulsion by the hydrophilic palisades, generally PEG, surrounding the core [5,38]. Thus, these characteristics suggested that this system possessed the potential to provide a feasible anti-cancer drug delivery system that might lead to improved biological performance *in vivo*.

4. Conclusions

In summary, TBIC micelles were prepared by polyion complexation of an anionic triblock copolymer, PLD-*b*-PEG-*b*-PLD, and a cationic drug, DOX, via electrostatic interactions. These micelles showed a narrow size distribution and incorporated a substantial amount of active drug in a reasonably stable manner. Moreover, they exhibited a pH-responsive release pattern that could facilitate delivery of a higher concentration of the drug to solid tumors. DOX-loaded TBIC micelles were significantly less cytotoxic to A-549 cells than free DOX, which was consistent with the sustained release of DOX from the carriers. Furthermore, DOX-loaded TBIC micelles were internalized into A-549 cells and they showed co-localization with Lysotracker® Green, which suggested that they reached late endosomes or lysosomes. Reduced clearance of micelle-delivered DOX from the circulation was observed *in vivo*. Based on these findings, it might be concluded that TBIC micelles comprising PLD-*b*-PEG-*b*-PLD showed excellent drug-delivery properties.

Table 1 – Pharmacokinetic parameters of DOX after intravenous administration of free DOX or TBIC micelles in rats (10 mg/kg).

	Free DOX	TBIC micelles
C_{max} (μg/mL)	6.54 ± 1.36	11.80 ± 2.28[a]
K_{el} (h^{-1})	0.97 ± 0.47	0.11 ± 0.03[a]
$t_{1/2}$ (h)	0.82 ± 0.32	6.46 ± 1.33[b]
AUC_{all} (μg min/mL)	7.21 ± 1.14	48.94 ± 2.53[b]
MRT (min)	1.64 ± 0.67	10.45 ± 2.66[b]

Data are presented as the mean ± SD ($n = 3$).
[a] $P < 0.05$ compared to the free DOX group.
[b] $P < 0.01$ compared to the free DOX group.

Acknowledgment

This research was supported by the National Research Foundation of Korea (NRF) grant funded by the Ministry of Education, Science and Technology (No. 2012R1A2A2A02044997 and No. 2012R1A1A1039059). We thank the Confocal Microscopy facility at WCU Nano Research Center of Yeungnam University for excellent technical assistance.

REFERENCES

[1] Cho HJ, Yoon IS, Yoon HY, et al. Polyethylene glycol-conjugated hyaluronic acid-ceramide self-assembled nanoparticles for targeted delivery of doxorubicin. Biomaterials 2012;33:1190–1200.
[2] Du JZ, Du XJ, Mao CQ, et al. Tailor-made dual pH-sensitive polymer-doxorubicin nanoparticles for efficient anticancer drug delivery. J Am Chem Soc 2011;133:17560–17563.
[3] Guan X, Li Y, Jiao Z, et al. A pH-sensitive charge-conversion system for doxorubicin delivery. Acta Biomater 2013;9:7672–7678.
[4] Kim JO, Kabanov AV, Bronich TK. Polymer micelles with cross-linked polyanion core for delivery of a cationic drug doxorubicin. J Control Release 2009;138:197–204.
[5] Amoozgar Z, Park J, Lin Q, et al. Low molecular-weight chitosan as a pH-sensitive stealth coating for tumor-specific drug delivery. Mol Pharm 2012;9:1262–1270.
[6] Maeda H, Wu J, Sawa T, et al. Tumor vascular permeability and the EPR effect in macromolecular therapeutics: a review. J Control Release 2000;65:271–284.
[7] Miyata K, Christie RJ, Kataoka K. Polymeric micelles for nano-scale drug delivery. React Funct Polym 2011;71:227–234.
[8] Bronich TK, Kabanov AV, Kabanov VA, et al. Soluble complexes from poly (ethylene oxide)-block-polymethacrylate anions and N-alkylpyridinium cations. Macromolecules 1997;30:3519–3525.
[9] Kabanov AV, Bronich TK, Kabanov VA, et al. Soluble stoichiometric complexes from poly (N-ethyl-4-vinylpyridinium) cations and poly (ethylene oxide)-block-polymethacrylate anions. Macromolecules 1996;29:6797–6802.

[10] Bronich TK, Keifer PA, Shlyakhtenko LS, et al. Polymer micelle with cross-linked ionic core. J Am Chem Soc 2005;127:8236–8237.
[11] Bronich TK, Nehls A, Eisenberg A, et al. Novel drug delivery systems based on the complexes of block ionomers and surfactants of opposite charge. Colloids Surf B Biointerfaces 1996;16:243–251.
[12] Burns NL, Emoto K, Holmberg K, et al. Surface characterization of biomedical materials by measurement of electroosmosis. Biomaterials 1998;19:423–440.
[13] Roser M, Fischer D, Kissel T. Surface-modified biodegradable albumin nano- and microspheres. II: effect of surface charges on in vitro phagocytosis and biodistribution in rats. Eur J Pharm Biopharm 1998;46:255–263.
[14] Rudt S, Müller R. In vitro phagocytosis assay of nano-and microparticles by chemiluminescence. I. Effect of analytical parameters, particle size and particle concentration. J Control Release 1992;22:263–271.
[15] Kamimura M, Kim JO, Kabanov AV, et al. Block ionomer complexes of PEG-block-poly(4-vinylbenzylphosphonate) and cationic surfactants as highly stable, pH responsive drug delivery system. J Control Release 2012;160:486–494.
[16] Batrakova EV, Li S, Reynolds AD, et al. A macrophage-nanozyme delivery system for Parkinson's disease. Bioconjug Chem 2007;18:1498–1506.
[17] Lee Y, Fukushima S, Bae Y, et al. A protein nanocarrier from charge-conversion polymer in response to endosomal pH. J Am Chem Soc 2007;129:5362–5363.
[18] Kakizawa Y, Kataoka K. Block copolymer micelles for delivery of gene and related compounds. Adv Drug Deliv Rev 2002;54:203–222.
[19] Ji M, Jin L, Guo J, et al. Formation of luminescent nanocomposite assemblies via electrostatic interaction. J Colloid Interface Sci 2008;318:487–495.
[20] Prakash S, Malhotra M, Shao W, et al. Polymeric nanohybrids and functionalized carbon nanotubes as drug delivery carriers for cancer therapy. Adv Drug Deliv Rev 2011;63:1340–1351.
[21] Shiraishi K, Kawano K, Maitani Y, et al. Polyion complex micelle MRI contrast agents from poly(ethylene glycol)-b-poly(l-lysine) block copolymers having Gd-DOTA; preparations and their control of T(1)-relaxivities and blood circulation characteristics. J Control Release 2010;148:160–167.
[22] Kataoka K, Harada A, Nagasaki Y. Block copolymer micelles for drug delivery: design, characterization and biological significance. Adv Drug Deliv Rev 2012;64:37–48.
[23] Kim JO, Ramasamy T, Yong CS, et al. Cross-linked polymeric micelles based on block ionomer complexes. Mendeleev Commun 2013;23:179–186.
[24] Kwon GS, Kataoka K. Block copolymer micelles as long-circulating drug vehicles. Adv Drug Deliv Rev 1995;16:295–309.
[25] Sun YL, Peng ZP, Liu XX, et al. Synthesis and pH-sensitive micellization of doubly hydrophilic poly(acrylic acid)-b-poly(ethylene oxide)-b-poly(acrylic acid) triblock copolymer in aqueous solutions. Colloid Polym Sci 2010;288:997–1003.
[26] Lavasanifar A, Samuel J, Kwon GS. Poly(ethylene oxide)-block-poly(L-amino acid) micelles for drug delivery. Adv Drug Deliv Rev 2002;54:169–190.
[27] Nakanishi T, Fukushima S, Okamoto K, et al. Development of the polymer micelle carrier system for doxorubicin. J Control Release 2001;74:295–302.
[28] Zhang L, He Y, Ma G, et al. Paclitaxel-loaded polymeric micelles based on poly(varepsilon-caprolactone)-poly(ethylene glycol)-poly(varepsilon-caprolactone) triblock copolymers: in vitro and in vivo evaluation. Nanomedicine 2012;8:925–934.
[29] Hecq JD, Lewis AL, Vanbeckbergen D, et al. Doxorubicin-loaded drug-eluting beads (DC Bead(R)) for use in transarterial chemoembolization: a stability assessment. J Oncol Pharm Pract 2013;19:65–74.
[30] Harada A, Kataoka K. Formation of polyion complex micelles in an aqueous milieu from a pair of oppositely-charged block copolymers with poly (ethylene glycol) segments. Macromolecules 1995;28:5294–5299.
[31] Yin H, Bae YH. Physicochemical aspects of doxorubicin-loaded pH-sensitive polymeric micelle formulations from a mixture of poly(L-histidine)-b-poly(ethylene glycol)/poly(L-lactide)-b-poly(ethylene glycol). Eur J Pharm Biopharm 2009;71:223–230.
[32] Missirlis D, Kawamura R, Tirelli N, et al. Doxorubicin encapsulation and diffusional release from stable, polymeric, hydrogel nanoparticles. Eur J Pharm Sci 2006;29:120–129.
[33] Porumb H. The solution spectroscopy of drugs and the drug-nucleic acid interactions. Prog Biophys Mol Biol 1978;34:175–195.
[34] Harada A, Kataoka K. Chain length recognition: core-shell supramolecular assembly from oppositely charged block copolymers. Science 1999;283:65–67.
[35] Bae Y, Kataoka K. Intelligent polymeric micelles from functional poly(ethylene glycol)-poly(amino acid) block copolymers. Adv Drug Deliv Rev 2009;61:768–784.
[36] Kim JO, Oberoi HS, Desale S, et al. Polypeptide nanogels with hydrophobic moieties in the cross-linked ionic cores: synthesis, characterization and implications for anticancer drug delivery. J Drug Target 2013;21:981–993.
[37] Kim JO, Sahay G, Kabanov AV, et al. Polymeric micelles with ionic cores containing biodegradable cross-links for delivery of chemotherapeutic agents. Biomacromolecules 2010;11:919–926.
[38] Kataoka K, Matsumoto T, Yokoyama M, et al. Doxorubicin-loaded poly(ethylene glycol)–poly(β-benzyl-l-aspartate) copolymer micelles: their pharmaceutical characteristics and biological significance. J Control Release 2000;64:143–153.